BRAIN CONNECTIVITY
Volume 6, Number 1, 2016

DOI: 10.1089/brain.2014.0328

Exercise Therapy for Parkinson's Disease: Pedaling Rate Is Related to Changes in Motor Connectivity

Chintan Shah,[1] Erik B. Beall,[2] Anneke M.M. Frankemolle,[3] Amanda Penko,[4] Michael D. Phillips,[2] Mark J. Lowe,[2] and Jay L. Alberts[3–5]

Abstract

Forced-rate lower-extremity exercise has recently emerged as a potential safe and low-cost therapy for Parkinson's disease (PD). The efficacy is believed to be dependent on pedaling rate, with rates above the subjects' voluntary exercise rates being most beneficial. In this study, we use functional connectivity magnetic resonance imaging (MRI) to further elucidate the mechanism underlying this effect. Twenty-seven PD patients were randomized to complete 8 weeks of forced-rate exercise (FE) or voluntary-rate exercise (VE). Exercise was delivered using a specialized stationary bicycle, which can augment patients' voluntary exercise rates. The FE group received assistance from the cycle. Imaging was conducted at baseline, end of therapy, and after 4 weeks of follow-up. Functional connectivity (FC) was determined via seed-based correlation analysis, using activation-based seeds in the primary motor cortex (M1). The change in FC after exercise was compared using linear correlation with pedaling rate. Results of the correlation analysis showed a strong positive correlation between pedaling rate and change in FC from the most affected M1 to the ipsilateral thalamus. This effect persisted after 4 weeks of follow-up. These results indicate that a plausible mechanism for the therapeutic efficacy of high-rate exercise in PD is that it improves thalamo-cortical connectivity.

Key words: exercise; functional connectivity; functional MRI; Parkinson's disease

Introduction

The "Shaking Palsy" first described by James Parkinson nearly 200 years ago is now known to be a neurodegenerative disease that affects 1.5% of adults over 65, worldwide (Meissner et al., 2011). There is no cure for Parkinson's disease (PD), and current medical and surgical therapies are for symptomatic control. As the disease progresses, the therapeutic window for medical therapies narrows with the increasing frequency of side effects. Deep brain stimulation is an effective therapy for late stage PD, but carries significant cost as well as risks due to the invasive procedure for placement of the device. This study focuses on forced-rate exercise (FE), a potential new, low-cost, and noninvasive therapy for PD, which has been shown to improve motor symptoms (Alberts et al., 2011; Ridgel et al., 2009).

Experiments in animal models of PD have shown that exercise can improve motor function and have a neuroprotective effect (Fisher et al., 2004; Petzinger et al., 2007, 2013; Tajiri et al., 2010; Tillerson et al., 2003; Zigmond et al., 2009). These animal models generally utilize either 1-methyl-4-phenyl-1,2,3,6-tetrahydropyridine (MPTP) or 6-hydroxydopamine (6-OHDA) lesioning to induce degeneration of dopaminergic neurons (Petzinger et al., 2013). Tillerson and colleagues (2003) showed that running rats on a treadmill after lesioning can preserve striatal dopamine and improve motor function, compared with rats that were not exercised. A later study by Poulton and Muir (2005) found that although dopamine levels were preserved, there were no improvements in motor function in the exercised rats. Tillerson and colleagues (2003) exercised the rats sooner after lesioning, and at a faster rate (Poulton and Muir, 2005). Other studies showing motor and neurochemical improvement also achieved high rates of exercise (Fisher et al., 2004; Petzinger et al., 2007). These results indicate that the rate of exercise may be important for the degree of effect seen.

[1]Department of Radiology, Hospital of the University of Pennsylvania, Philadelphia, Pennsylvania.
[2]Imaging Institute, Cleveland Clinic, Cleveland, Ohio.
[3]Department of Biomedical Engineering, Case Western Reserve University, Cleveland, Ohio.
[4]Center for Neurological Restoration, Cleveland Clinic, Cleveland, Ohio.
[5]Cleveland FES Center, L. Stokes Cleveland VA Medical Center, Cleveland, Ohio.

Attempts to reproduce these results in human studies of exercise have had mixed results (Smidt et al., 2005). The apparent inconsistency between human and animal studies is likely related to differences in the type of exercise performed. In animal studies, the subject is forced to exercise at a rate greater than its voluntary exercise rate, whereas in human studies, the subjects exercise at their voluntary rate. The ensuing hypothesis raised in a subsequent study was that FE would improve motor symptoms compared to voluntary-rate exercise (VE) (Ridgel et al., 2009). FE is defined as exercise at a rate above a subject's voluntary (preferred) rate, maintained using an external system (Ridgel et al., 2009). In this initial study, FE was delivered via tandem bicycle with the patient behind a personal trainer (Ridgel et al., 2009). For further study of FE, our laboratory developed a motor driven stationary cycle that can augment the rider's pedaling rate (see Methods section) (Beall et al., 2013). The cycle monitors multiple physiologic and exercise-related variables including heart rate and rider-generated power, allowing manipulation of rate and intensity semi-independently. For example, if a patient is cycling at the desired pedaling rate but his heart rate begins to exceed his target heart rate (THR) range (see Methods section), the cycle can increase the power contribution from the motor, in turn decreasing patient-generated power to maintain the same pedaling rate, or automatically reduce the resistance to pedaling.

Ridgel and associates (2009) compared the effects of FE and VE on the symptoms of PD patients in a randomized study of 10 patients. The average pedaling rate in the FE group was 43% greater than that in the VE group, and aerobic intensity was matched between groups. After completing 8 weeks of bicycle exercise, those patients randomized to FE showed 35% improvement in clinical motor ratings, while patients randomized to VE did not show improvement (Ridgel et al., 2009). Other studies have found that improvements in corticomotor excitability and motor performance may be related to the intensity of exercise (Fisher et al., 2008), and that patients undergoing intensive exercise showed increases in striatal dopamine D2 receptor binding potential measured with positron emission tomography (PET) imaging (Fisher et al., 2013). The mechanism underlying this rate-dependent effect is not fully understood. The goal of this study is to understand how the neural network changes that occur after exercise are related to the rate of that exercise.

Functional connectivity magnetic resonance imaging (fcMRI) is used in this study to better understand this relationship. We define fcMRI as blood oxygenation level-dependent (BOLD)-weighted MRI, during which the subject stimulus (or lack thereof) is constant throughout the entire acquisition. In resting-state fcMRI (Biswal et al., 1995; Lowe, 2012; Lowe et al., 1998), BOLD-weighted MRI data is acquired of the brain while the patient remains at rest, with no change in stimuli. If the subject is not in a resting state, but instead performing a continuous-task, low frequency BOLD fluctuation (LFBF) correlations among regions of the task-related network are altered (Biswal and Hyde, 1998; Lowe et al., 2000). In continuous task fcMRI scan, the subject must perform a task continuously throughout the entire scan, and perform it at a frequency above the LFBF cutoff frequency (0.08 Hz).

The study of functional connectivity (FC) in PD is relatively young (Baudrexel et al., 2011; Göttlich et al., 2013; Hacker et al., 2012; Helmich et al., 2010; Luo et al., 2014; Poston and Eidelberg, 2012; Sharman et al., 2013; Wu et al., 2009, 2011a, 2012; Yu et al., 2013). An early study evaluating resting-state FC (rsFC) in PD showed that rsFC between the pre-supplementary motor area (pre-SMA) and putamen was decreased, whereas that between the pre-SMA and primary motor cortex (M1) was increased (Wu et al., 2011a). A recent study of striatal connectivity in PD patients (on medication) found decreased striatal connectivity to the extended brainstem, and weaker anticorrelations to the sensorimotor cortex, compared with normal controls (Hacker et al., 2012). Sharman and colleagues (2013) evaluated both anatomical and FC, and found that PD patients had decreased rsFC from the thalamus to the sensorimotor cortex, globus pallidus, and substantia nigra, which corresponded to decreases in anatomical connectivity. Despite some differences among these studies, a common finding in PD patients is decreased connectivity between subcortical and cortical motor areas, and increased in connectivity between cortical motor areas that compensate for these deficits. In a recent cross-sectional study in our laboratory evaluating connectivity changes after a single session of exercise, we found that medication and FE have a similar effect on motor connectivity in PD (Beall et al., 2013). Thus, we hypothesized that exercise rate-related changes in connectivity would manifest as tending to improve the deficits in subcortical-cortical connectivity.

To investigate the rate-dependence of exercise-related changes in connectivity, we undertook a study in which PD patients were randomized to complete 8 weeks of forced-rate or voluntary-rate bicycle exercise. Changes in connectivity with the M1 were then analyzed, as a function of pedaling rate, to determine the effect of exercise therapy on FC in PD. We show that pedaling rate is highly correlated to certain changes in motor connectivity after exercise.

Methods

Experimental overview

Patients were consented and enrolled, and baseline studies were conducted including clinical evaluation, MRI imaging, and cardiovascular testing (described below), in a protocol approved by the Cleveland Clinic Institutional Review Board. Subjects were randomized to either FE or VE. The study involved an 8-week period in which the randomly assigned exercise intervention occurred, and a 4-week follow-up period without intervention, during which patients were asked to return to their normal activity levels. MRI imaging was done at baseline, after 8 weeks of therapy (end of therapy [EOT]), and 4 weeks thereafter (end of therapy +4 weeks of follow-up [EOT +4]). The patients included in this study were the subset of patients who underwent both exercise and imaging within in a larger clinical trial of forced exercise.

Study sample

Twenty-seven patients with mild-to-moderate idiopathic PD were enrolled in the study and underwent both exercise and imaging. Primary inclusion criteria included the

following: clinical diagnosis of idiopathic PD, age between 30 and 65 years, not currently engaged in formal exercise intervention or clinical study, and Hoehn and Yahr stage II–III (Hoehn and Yahr, 1967) when off PD medication. Primary exclusion criteria included the following: existing cardiopulmonary disease or stroke, presence of dementia, and any medical or musculoskeletal contraindications to exercise. Potential study candidates were prescreened with the American Heart Association exercise preparticipation questionnaire (Balady et al., 1998), to exclude those with major signs or history of cardiovascular or pulmonary disease. MRI-related exclusion criteria included the following: severe claustrophobia, health concerns with exposure to the magnetic fields, or MRI-incompatible metal implant.

Exercise intervention

Before randomization, patients underwent cardiopulmonary exercise fitness testing on a cycle ergometer, with EKG and blood pressure monitoring, to ensure adequate exercise tolerance and determine their baseline voluntary exercise rate. After randomization to VE or FE, patients underwent three exercise sessions per week, separated by at least 1 day, for 8 weeks. The aerobic exercise intensity was matched for both groups, as the THR for patients in both groups was in the range of 60–80% of the age-predicted maximum (220 minus patient's age) (Karvonen et al., 1957). Each session comprised a 10-min warm up and cool down period, separated by a 40 min main exercise set, during which patients were instructed to keep their heart rate in their THR. Initially, the 40 min main exercise set included ''on the bike'' rest breaks of 2 min, every 10 min. Additional breaks were allowed if requested. This progressed to two 20 min sessions, separated by a 2 min break, by 4 weeks into the exercise period.

To deliver forced exercise, a specialized stationary cycle was developed that includes a motor driven pedal system that can augment patients' voluntary exercise rate, and which monitors heart rate, power produced by the subject, power contribution of the motor, cadence (pedaling rate), exercise time, and ambient temperature, among other variables. The motor is controlled by a feedback mechanism responsive to pedaling rate, patient work, and heart rate. We are currently completing an engineering white paper in which the specifications of the exercise cycle, motor parameters, and interface will be detailed.

Subjects in the VE group operated the cycle without motor assistance, and voluntarily determined their resistance level and cadence. Subjects in the FE group received a variable degree of motor assistance to pedal at a rate at least 35% greater than their voluntary rate, as determined by the preliminary fitness testing. Both groups were instructed to maintain their heart rate in the THR.

MRI data acquisition

Patients underwent scanning on three occasions: at baseline, EOT, and EOT +4. Although subjects were on PD medication for the duration of the study, scans were conducted while the patients were off medication for 12 h. Subjects were scanned using a 12 channel receive-only head coil in a Siemens Trio 3T scanner (Siemens Medical Solutions, Erlangen, Germany), with the use of a bite bar to reduce head motion. During each session, scans included.

Scan 1: anatomic 3D whole-brain T1 study: T1-weighted inversion recovery turboflash (MPRAGE). One hundred twenty axial slices; thickness = 1.2 mm; field of view (FOV) = 256 × 256 mm; inversion time (TI)/echo time (TE)/repetition time (TR)/flip angle (FA) = 1900 msec/1.71 msec/900 msec/8°.

Scan 2: functional MRI motor activation study. One hundred sixty repetitions of thirty-one 4 mm thick axial slices acquired using a pulse sequence based on the prospective motion-controlled, gradient-recalled echo, echoplanar acquisition (Thesen et al., 2000); TE/TR/FA = 29 msec/2800 msec/80°; matrix = 128 × 128; FOV = 256 × 256 mm; bandwidth = 250 kHz. Patients were instructed to perform the complex finger tapping task described below.

Scan 3: fcMRI continuous-task connectivity study. Whole-brain LFBF fcMRI study. One hundred thirty-seven repetitions of thirty-one 4 mm thick axial slices; TE/TR = 29/3000 msec; matrix = 128 × 128; FOV = 256 × 256 mm; receive bandwidth = 250 kHz. The subject performed a force-tracking motor task with the most affected hand (MAH) during the entire scan, as described below.

Scan 4: fcMRI resting-state connectivity study. Whole-brain LFBF fcMRI study. The purpose of this study was analysis of the continuous-task connectivity data from scan 3, as it relates to pedaling rate in PD patients undergoing exercise therapy. However, resting-state connectivity data was also acquired using the same protocol as scan 3, but with the subject resting comfortably with eyes closed rather than performing a task.

The subjects performed the following tasks during scanning.

Complex bilateral finger tapping task. The task was performed with a pair of fiber optic data gloves (Fifth Dimension Technologies, Irvine, CA). Data were collected and synchronized with MRI scanning using an acquisition system designed and built in-house (Lowe et al., 2008). Subjects performed a bilateral complex finger tapping task beginning with a 60 sec rest period, followed by four ''on/off'' cycles, each of which comprised 45 sec of tapping and 45 sec of rest (hereinafter ''block paradigm''). This task was performed during scan 2 above.

Continuous fingertip force tracking task. This task was performed using a customized pinch grip force dynamometer system designed in house (Beall et al., 2013). Data were acquired at 128 Hz. Subjects applied a pinch grip (thumb and index finger only) to the device with their MAH to generate force readings. Immediately before each scanning session, each subject's maximum voluntary contraction force (MVC) was measured using the dynamometer as the average of three trials of 5 sec each, separated by at least 1 min. Each subject's target force was set at 5% MVC. During the task, subjects were given real-time feedback of their applied force relative to the target and instructed to maintain the target force for the entirety of the scan. Subjects were trained and identical practice trials were conducted before scanning to ensure comprehension and minimize differences in practice effect. Task performance was analyzed to establish minimum performance criteria for both tasks.

Image postprocessing

The functional MRI (fMRI) and fcMRI data were postprocessed in a manner similar to Lowe et al. (2008), including the following steps:

1. Retrospective motion correction using the AFNI 3dvolreg routine (Cox, 1996). This step aligns all volumes in a four-dimensional (4D) data set with the initial volume, and produces a 6 degree of freedom set of motion parameters for each volume that is used in later correction and analysis.
2. Physiologic (cardiac and respiratory) noise source estimation and regression using PESTICA (Beall and Lowe, 2007, 2010).
3. Voxel-specific second-order motion correction to correct for the effects of voxel-level motion (Beall et al., 2013; Bullmore et al., 1999).
4. Spatial filtering with a 4-mm full width at half-maximum (FWHM) Gaussian in-plane filter. Such spatial filtering is generally not needed at 3T because it unnecessarily decreases spatial resolution. If it is done, a Hamming filter should be used because it is a matched filter designed to increase the signal-to-noise ratio (Lowe and Sorenson, 1997). The design of this study was such that each subject's seed voxel for FC analysis was propagated to all of their time points via coregistration, which can result in partial volume effects at the voxel-level and a resultant shift in the seed by up to one voxel. Thus, a 4-mm FWHM Gaussian blur was chosen to allow spatial coherence between study time points without significantly degrading the spatial resolution of the data.
5. (fcMRI data only) Temporal filtering to remove all fluctuations above 0.08 Hz (Biswal et al., 1995; Lowe et al., 1998).

Motion analysis

Second-order motion correction. The motion parameters generated from the retrospective motion correction (postprocessing step 1) were used to trigonometrically calculate the x, y, z, and total displacement at each voxel (Bullmore et al., 1999; Jiang et al., 1995). These displacements and certain parameterizations of them are known to correlate with signal change caused by motion and are regressed from the signal (Bullmore et al., 1999). This method was applied to all fMRI and fcMRI scans, in a manner similar to Beall et al. (2013).

Peak to peak displacement exclusions. Motion parameters were also used to calculate the head displacement in each frame and subtracted to find the peak-to-peak displacement in the fcMRI data (Jiang et al., 1995). Any study with a peak to peak displacement above 1.2 mm at any time during the scan was excluded from further analysis.

Quality assessment of FC maps. Once FC maps were generated (see Methods section: fcMRI data analysis), they were evaluated for motion artifact using a combination of visual assessment and statistical characterization (see Appendix), and those with significant artifact were excluded from further analysis.

Image analysis

All activation and FC maps were created in native scan space, and then transformed to a common space for further analysis. To do so, each activation map from the three study time points is first coregistered to a common temporary space, seed voxels defined here, and this seed is transformed back to the native scan space of the FC scans at each study time point and inspected for quality. Here, we describe this procedure.

fMRI data analysis. The fMRI data were analyzed by computing a least squares fit of the block paradigm described earlier to the time series data at each voxel (Lowe and Russell, 1999). This resulted in a whole-brain Student's t map, which was thresholded to determine regions of significant involvement in the complex bilateral finger tapping task. For each subject, fMRI data from all study time points (Baseline, EOT, EOT +4) were coregistered to the baseline scan, and this coregistration was applied to the activation maps. The maps were then averaged to create a single average activation map for each subject, which was used for seed localization in the FC analysis.

fcMRI data analysis. FC analysis was done using the seed-based correlation method with the seed defined by activation, similar to the methods used in Lowe et al. (2002, 2008). The FC analysis involved was as follows:

1. Regions of interest (ROIs) were manually drawn for the left and right hand areas of the M1 based on both anatomical location and activation strength. These were drawn for each individual activation map and combined across each subject's multiple study time points via coregistration and a logical OR operator. The final ROIs were used in combination with the average activation map for seed selection.
2. Seed voxels were selected as the single voxel with the largest average activation within each ROI, after the ROIs and average activation map were coregistered to the subject's baseline fcMRI data.
3. Seed voxels were then propagated to the later fcMRI scans via coregistration. This was performed so that the seed would represent the same anatomical region in every follow-up study of that subject.
4. A reference time series was produced by calculating the arithmetic average of the time series' of the seed voxel and the eight surrounding in-plane voxels in the fcMRI dataset.
5. The reference time series was correlated with the time series at every voxel in the brain, and the correlation coefficient converted to a Student's t statistic (Press et al., 2007).
6. The Student's t map is z-score corrected by fitting a normal distribution to the FWHM of the distribution of Students t scores for all voxels as described in Lowe et al. (1998).

The result is a whole-brain map of z-scores representing FC to the seed region (FC map).

Second level statistical analysis

Spatial normalization into Talairach space. To perform group level analyses, FC maps were registered into a common space. The fcMRI datasets were coregistered with the

anatomical images acquired in scan 1 using local Pearson correlation (Saad et al., 2009). Anatomical images were normalized into the standard Talairach-Tournoux space using the AFNI auto-Talairach tool in combination with a modified template developed in house to correctly align the anterior commissure-posterior commissure line (Mathew, 2012). These transformations were then applied to the FC maps to normalize them into Talairach space, which involved resampling to $1 \times 1 \times 1$ mm resolution. Normalized FC maps were then spatially smoothed with a 6-mm FWHM Gaussian filter in preparation for group-level analysis.

Effect of exercise rate on FC. To determine the change in FC from baseline, difference maps were created by subtracting the baseline FC map from the EOT or EOT +4 map (i.e., $\Delta FC_{EOT} = FC_{EOT} - FC_{Baseline}$). These could only be calculated if neither FC map had been excluded. Since patients performed the task with the MAH, Right M1 FC maps were used for patients with Left MAH, and vice versa. For patients with Right MAH, the Left M1 FC maps were mirrored to allow group-level analysis across all patients. Thus, these maps represent FC to the most affected M1 (*M1), but these are all *displayed* as connectivity to the right motor cortex. The ΔFC maps were concatenated into a 4D dataset (3D× subject) and voxel-wise correlations were then performed with cadence, after adjusting for age, to determine regions in which ΔFC was related to the subject's average pedaling rate. The correlation measure used was a Student's *t* statistic. Correction for multiple comparisons across voxels was performed using a family wise error correction, computed via a 10,000 iteration Monte Carlo simulation, to determine significant cluster sizes. The significance level was set at $p < 0.05$, corrected.

In this study, we sought to elucidate rate-related changes in connectivity. Patients were randomized to FE versus VE such that the FE group should have a substantially greater pedaling rate. In the initial study (Ridgel et al., 2009), patients in the FE group pedaled 43% faster than those in the VE group (86 vs. 60 rpm), resulting in improvements in clinical motor ratings. Based on these findings, we had set the forced rate in our study to be 35% greater than the patient's own voluntary rate, and expected a similar difference in pedaling rates between groups. However, due to variability in patients' baseline rates, this did not translate to a sufficient group difference in pedaling rates (19% greater pedaling rate in the FE vs. VE group, 86 vs. 73 rpm, with substantial overlap in pedaling rates). For this reason, we allowed the independent variable to be the downstream continuous variable—pedaling rate—to directly elucidate the relationship between pedaling rate and connectivity via correlation, rather than indirectly via group comparisons.

Results

Study sample

Twenty-seven patients were randomized to the VE ($n = 14$) or FE ($n = 13$) groups. All subjects underwent the 3 scanning sessions, except one patient who was lost to follow-up after EOT and underwent only the first two sessions, bringing the total number of scanning sessions to 80. During 1 of these 80 sessions, fcMRI data could not be acquired due to technical difficulties. During another two sessions, the datasets were corrupted with spikes and could not be used.

Subject demographics are presented in Table 1. Both groups were comparable with respect to age, gender, handedness, laterality of MAH, disease duration, medication (levodopa equivalent daily dose [LEDD]), and baseline disease burden as measured by the Unified Parkinson's Disease Rating Scale (UPDRS) III—motor score. The pedaling rates of the two groups were statistically different, as discussed above in the Methods section.

Task performance analysis

Performance in the complex bilateral finger tapping task was above minimum criteria during all scanning sessions except for 1 of 80 scans, which was excluded from further analysis. Since seeds were chosen from average fMRI activation maps (averaged over the study time points), this did not exclude any patients from the analysis. The continuous fingertip force tracking task was performed adequately during all except for one scanning session, in which the patient did not adequately maintain the target force. This scan was not included in the group analysis. All patients performed the task at a frequency above the LFBF cutoff frequency.

Motion analysis

The implementation of second-order motion correction resulted in all fMRI activation maps being suitable for seed selection for the connectivity analysis. Peak-to-peak motion exclusions resulted in the exclusion of five fcMRI scans. Quality assessment of the FC maps using statistical characterization (see Appendix) led to the identification of seven left-M1 and five right-M1 FC maps that did not adequately

Table 1. Characteristics of Study Subjects

	VE group (n = *14*)	*FE group* (n = *13*)	p	*Test*
Mean age (SD)	57.2 (7.1)	56.5 (9.5)	0.84	Two sample *t*-test
No. of females, *n* (%)	5 (36)	5 (38)	1	Fisher exact test
No. of dominant hand = R, *n* (%)	12 (86)	13 (100)	0.48	Fisher exact test
No. of most affected hand = R, *n* (%)	8 (57)	3 (23)	0.13	Fisher exact test
Median no. of months PD (IQR)	45.5 (15–86.1)	36 (17.7–61.3)	0.61	Wilcoxon Rank sum
Median LEDD (IQR)	600 (400–750)	303 (100–723)	0.13	Wilcoxon Rank sum
Mean baseline UPDRS III motor (SD)	23.3 (11.4)	26.5 (7.8)	0.42	Two sample *t*-test
Mean cadence (SD)	72.66 (12.24)	86.12 (6.52)	0.002	Two sample *t*-test

FE, forced-rate exercise; IQR, interquartile range; LEDD, levodopa equivalent daily dose; PD, Parkinson's disease; SD, standard deviation; UPDRS, Unified Parkinson's Disease Rating Scale; VE, voluntary-rate exercise.

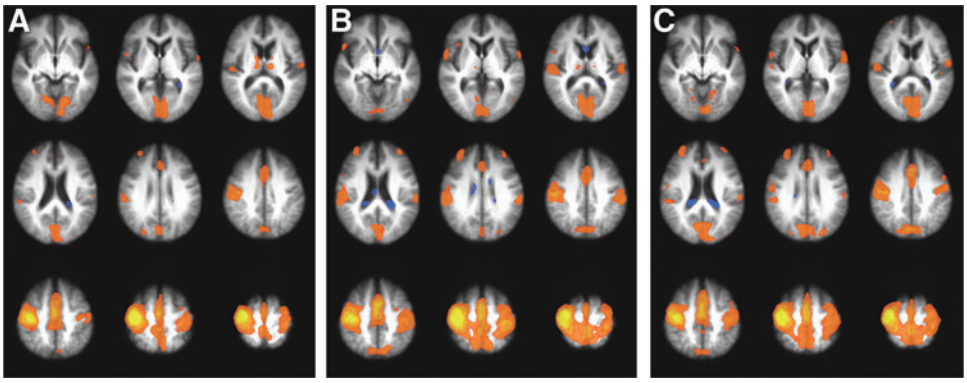

FIG. 1. Average functional connectivity (FC) map of all patients at **(A)** baseline, **(B)** end of therapy (EOT), and **(C)** end of therapy +4 weeks (EOT +4). Most affected primary motor cortex (*M1) is displayed on the radiological right side (image left). *z* Coordinates of slices shown: −1, 7, 15, 23, 31, 39, 47, 55, 63.

represent motor connectivity. Three of these maps corresponded to the patients' most affected side, and were excluded from further analysis. For two subjects in the FE group, the EOT +4 map was excluded, and for one subject in the VE group, the baseline map was excluded (thus, the subject could not be included at either time point). The final numbers of subjects included in each analysis after all exclusions are listed in the figure captions.

Effect of exercise rate on FC changes

FC maps of the motor network were created as described for each patient. For illustrative purposes, the group average FC map at each time point is shown in Figure 1.

Student's *t* maps for the effect of pedaling rate were generated as described and thresholded/clustered. This identified regions in which the change in that region's task related FC with the *M1 (ΔFC) was significantly related to cadence, after adjusting for age. Positive and negative correlations are displayed as orange and blue regions in the correlation maps, respectively. Stronger correlation is indicated by a brighter color. The final numbers of subjects included in each correlation analysis (after exclusions) are listed in the figure captions.

Figure 2 shows regions in which ΔFC from baseline to EOT (ΔFC_{EOT}) is significantly related to cadence. The task related FC between the *M1 and the ipsilateral thalamus tended to increase in those who cycled faster, whereas that

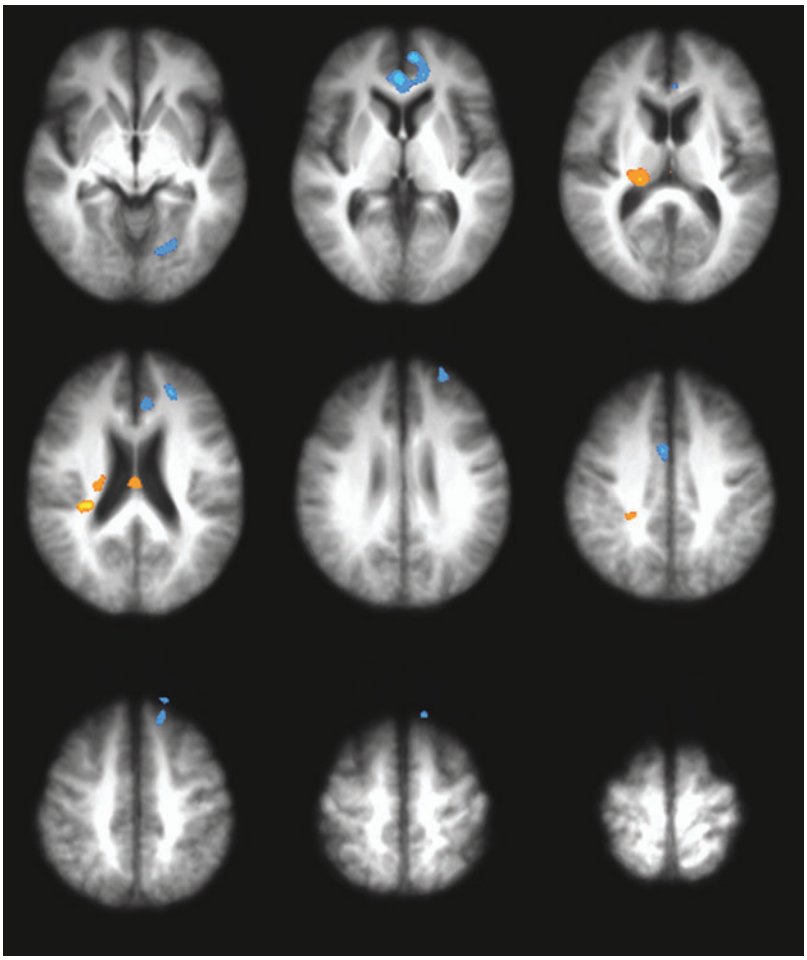

FIG. 2. Correlation map of ΔFC_{EOT} with cadence. Colored regions represent those in which changes in task-related FC to the *M1 (at EOT) are correlated with cadence. *M1 is displayed on the radiological right side (image left). $N = 20$. Clusters are significant to $p < 0.05$, family wise error (FWE) corrected. *z* Coordinates of slices shown: −1, 7, 15, 23, 31, 39, 47, 55, 63.

Table 2. Coordinates of Clusters Showing Significant Correlation Between Cadence and Change in FC with *M1 at EOT

Cluster	*No. of voxels*	*Coordinates*			*Location*[a]
		x	y	z	
1	1702	−2.6	39.2	7.1	Left anterior cingulate
2	1076	20.5	−21.2	17.8	Right thalamus
3	731	−18.4	−65.5	3.2	Left lingual gyrus
4	662	−21.7	43.6	26.4	Left superior frontal gyrus
5	573	−5.7	31.5	21.4	Left anterior cingulate
6	567	−12.7	59.8	−9.7	Left superior frontal gyrus
7	566	−14.6	36.1	50	Left superior frontal gyrus
8	539	3	3.9	36.9	Right cingulate gyrus
9	510	30.7	−29.5	24	Right insula
10	506	1.6	−17.8	19.9	Right thalamus
11	449	23.4	−34.9	35.7	Right cingulate gyrus

[a]Note that the most affected side is displayed as the right side; right indicates ipsilateral to the most affected side, left indicates contralateral.

EOT, end of therapy; FC, functional connectivity; *M1, most affected primary motor cortex.

between *M1 and the medial prefrontal cortex tended to decrease. The thalamic effect was strongest in the posterolateral region of the ventral thalamus, but was also seen in the dorsomedial thalamus. Significant clusters at EOT are listed in Table 2. At EOT +4, after 4 weeks of follow-up, the positive correlation in the thalamus was preserved (Fig. 3). A trend toward positive correlation was also seen in the contralateral motor cortex, while a trend toward negative correlation was seen in the SMA. Significant clusters at EOT +4 are listed in Table 3.

To provide an improved visualization of the relationship, the ΔFC values for each patient were extracted from the

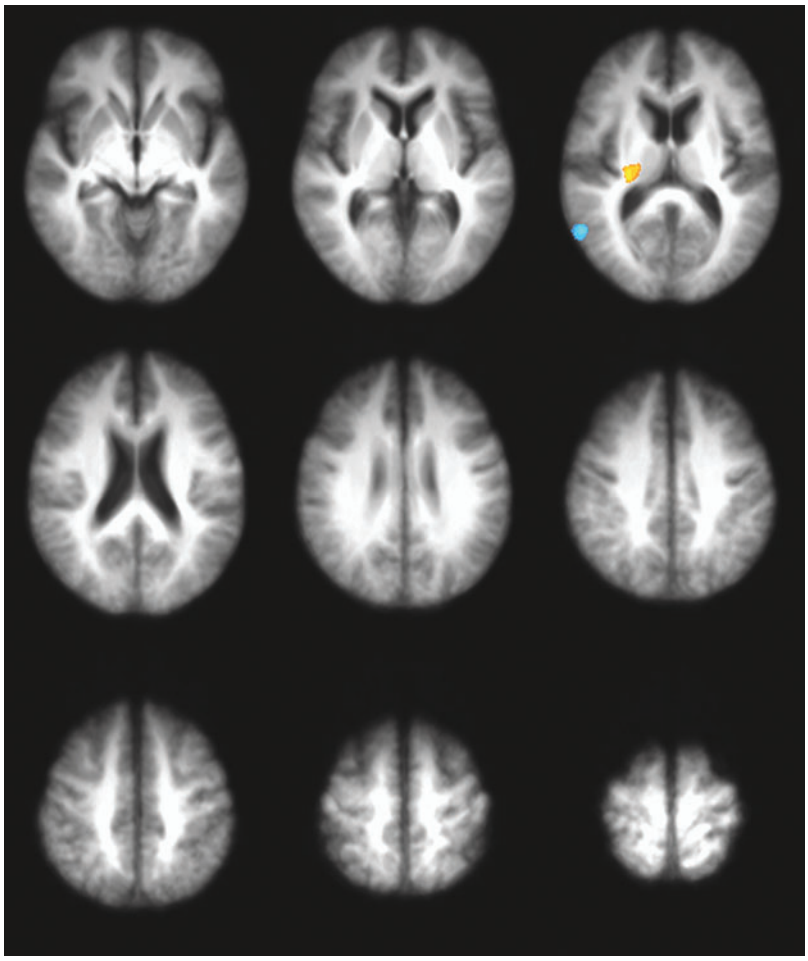

FIG. 3. Correlation map of $\Delta FC_{EOT\ +4}$ with cadence. Colored regions represent those in which changes in task-related FC to the *M1 (at EOT +4) are correlated with cadence. *M1 is displayed on the radiological right side (image left). $N = 18$. Clusters are significant to $p < 0.05$, FWE corrected. z Coordinates of slices shown: −1, 7, 15, 23, 31, 39, 47, 55, 63.

Table 3. Coordinates of Clusters Showing Significant Correlation Between Cadence and Change in FC with *M1 at EOT +4

Cluster	No. of voxels	Coordinates x	y	z	Location[a]
1	547	55.9	−55.9	15.4	Right superior temporal gyrus
2	535	24.6	−19.6	15.5	Right thalamus

[a]Note that the most affected side is displayed as the right side; right indicates ipsilateral to the most affected side, left indicates contralateral.

EOT +4, end of therapy +4 weeks of follow-up.

ΔFC maps in the region of high correlation in the thalamus at EOT and EOT +4. These were adjusted for age (the effect of age was regressed out), and the adjusted ΔFC values were plotted against cadence in Figure 4. There is a strong correlation at both time points, and patients who pedaled above 75–80 rpm were more likely to show increases in thalamo-cortical connectivity.

Discussion

The primary aim of this study was to investigate the rate-related neural network changes that occur with exercise in PD using fcMRI. We found that PD patients who pedaled faster during their 8 weeks of exercise tended to have increases in cortico-subcortical connectivity *during task performance* compared to those who pedaled slower. The *active* motor cortex in these patients showed a stronger connection to the ipsilateral thalamus (and a trend toward stronger connection to the putamen) after 8 weeks of exercise therapy. This effect persisted 4 weeks after the end of the exercise period.

The region of the thalamus in which the high correlation is seen is a large posterior area, ranging from posterolateral at the ventral aspect to more medial dorsally. These areas likely include the pulvinar nucleus and the posterior aspect of the ventrolateral nucleus. The ventrolateral nucleus serves as a thalamic relay nucleus for the motor circuit, receiving input from the basal ganglia and cerebellum, and directing output to motor cortical regions (Nolte, 2009). The pulvinar nucleus is an association nucleus of the thalamus that connects largely to the parietal, occipital, and temporal association cortices (Nolte, 2009). This is consistent with the fact that improved connectivity to the pulvinar region was seen *during* the performance of a visuomotor feedback task, in which the subject must integrate visual sensory information to modulate his/her motor output. Thus, in patients who pedal faster, there tends to be improvement in thalamo-cortical task-related connectivity, specifically in regions of the thalamus important for motor control and sensory integration.

Such task-related FC is not as commonly studied as resting-state FC, though several groups have published measures of effective connectivity (EC) during a task (Helmich et al., 2009; Palmer et al., 2009, 2010; Wu et al., 2010, 2011b). EC differs from FC in that it is measured during a traditional fMRI scan (i.e., with alternating task blocks), rather than in what we refer to as an fcMRI scan, in which the subject is in a constant state throughout the entire scan. Further, EC measures the degree to which the activity of one region contributes to another (Wu et al., 2011b). A study of particular interest is that by Palmer et al. (2010) as the force tracking device and task used was similar to that of this study, though it was applied in a block design. They reported that EC during the task in PD patients was decreased in the striato-thalamo-cortical pathway, and increased in the cerebello-thalamo-cortical pathway, relative to normal controls (Palmer et al., 2010). Wu and associates (2011b) reported similar findings of EC during a self-initiated finger tapping task. They found that task-related EC between the putamen and cortical motor areas was decreased compared with normal controls, and was inversely associated with UPDRS (a higher UPDRS score indicates greater symptom burden). They also reported that EC between M1 and the pre-SMA, premotor cortex, parietal cortex, and cerebellum was increased relative to controls, and positively related to UPDRS (Wu et al., 2011b). The increases in cortical-cortical EC are proposed to be compensatory mechanisms for the decreases in subcortical-cortical EC (Palmer et al., 2010; Wu et al., 2011b). These findings are consistent with our observation of a tendency for increases in subcortical-cortical task-related FC in patients who pedal faster. This implies that a plausible mechanism for the therapeutic efficacy of exercise in PD is that it improves thalamo-cortical connectivity during the performance of a task.

This study was limited by relatively small sample size. This may be responsible for the regions that did not meet statistical significance at one time point, but did at another. A second limitation was the degree of motion in the studies;

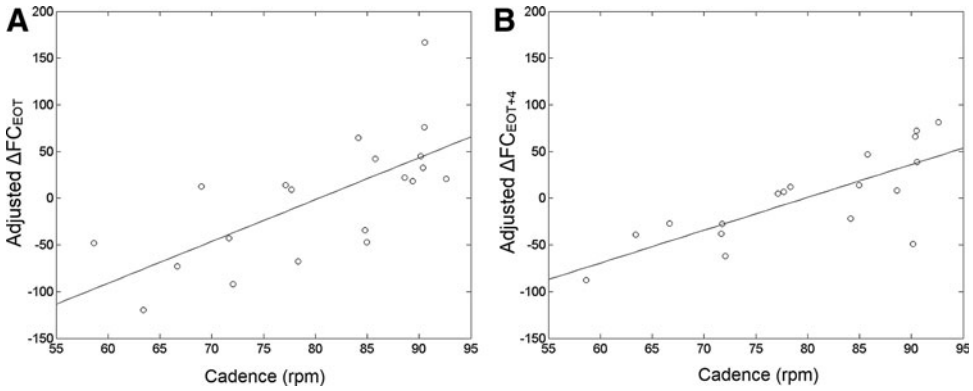

FIG. 4. Plot of cadence versus change in FC between *M1 and the thalamus, adjusted for age, at **(A)** EOT, and **(B)** EOT +4. FC is presented in units of *z*-score ×100.

several studies had to be excluded due to motion. This is an important problem in neuroimaging research in PD. To reduce the impact of motion, we incorporated more sophisticated motion correction methods, such as voxel-specific second-order motion correction, which is more effective than volumetric (non-voxel-specific) second-order motion correction. Motion was reduced by the use of a bite-bar during the MRI sessions, resulting in only a few scans with more than 1.2 mm motion. This threshold is not ideal, but we stress that it is much lower than commonly applied thresholds. We believe a simpler task could reduce motion further. A third limitation was the lack of an on-medication scanning session. Previous work in our laboratory has shown that the effects of PD medication and exercise on FC are related (Beall et al., 2013), and thus an on-medication scan would be useful in an analysis of exercise and FC. Thus, ongoing and future work does involve larger sample sizes, an on-medication scanning session, and a simplification of the scanning protocol to lower the degree of motion.

Conclusion

This work provides important insight into the mechanism of the therapeutic effect of exercise in PD. The effect may be driven by strengthening of thalamo-cortical connectivity during task performance. These connectivity changes are associated with pedaling rate during exercise, and are greater in those who pedal faster. We conclude that increases in thalamo-cortical motor connectivity are directly related to pedaling rates of patients undergoing exercise therapy for PD, and thus these connectivity changes may underlie the rate-dependent efficacy of exercise therapy.

Acknowledgments

Funding for this study was provided by NIH/NINDS, and VA Merit Review. Additional support for C.S. was provided by the Parkinson's Disease Foundation and the American Parkinson's Disease Association. We would also like to acknowledge the Cleveland Clinic Lerner Research Institute and Mellen Center staff who helped and contributed to this study: John Cowan, Amy (Liz) Jansen, Blessy Matthew, Katherine Murphy, and Derrek Tew.

Author Disclosure Statement

J.L.A. has authored intellectual property related to the motor control algorithm of the forced-exercise cycle. Otherwise, no competing interests exist.

References

Alberts JL, Linder SM, Penko AL, Lowe MJ, Phillips M. 2011. It is not about the bike, it is about the pedaling: forced exercise and Parkinson's disease. Exerc Sport Sci Rev 39:177–186.

Balady GJ, Chaitman B, Driscoll D, Foster C, Froelicher E, Gordon N, Pate R, Rippe J, Bazzarre T. 1998. Recommendations for cardiovascular screening, staffing, and emergency policies at health/fitness facilities. Circulation 97:2283–2293.

Baudrexel S, Witte T, Seifried C, von Wegner F, Beissner F, Klein JC, Steinmetz H, Deichmann R, Roeper J, Hilker R. 2011. Resting state fMRI reveals increased subthalamic nucleus-motor cortex connectivity in Parkinson's disease. Neuroimage 55:1728–1738.

Beall E, Lowe M, Alberts JL, Frankemolle AM, Thota AK, Shah C, Phillips MD. 2013. The effect of forced-exercise therapy for Parkinson's disease on motor cortex functional connectivity. Brain Connect 3:190–198.

Beall EB, Lowe MJ. 2007. Isolating physiologic noise sources with independently determined spatial measures. Neuroimage 37:1286–1300.

Beall EB, Lowe MJ. 2010. The non-separability of physiologic noise in functional connectivity MRI with spatial ICA at 3T. J Neurosci Methods 191:263–276.

Beall EB, Lowe MJ. 2014. SimPACE: generating simulated motion corrupted BOLD data with synthetic-navigated acquisition for the development and evaluation of SLOMOCO: a new, highly effective slicewise motion correction. Neuroimage 101:21–34.

Biswal B, Yetkin FZ, Haughton VM, Hyde JS. 1995. Functional connectivity in the motor cortex of resting human brain using echo-planar MRI. Magn Reson Med 34:537–541.

Biswal BB, Hyde JS. Functional Connectivity During Continuous Task Activation. In Proceedings of the 6th ISMRM, Sydney, Australia, 1998, p. 1410.

Bullmore ET, Brammer MJ, Rabe-Hesketh S, Curtis VA, Morris RG, Williams SC, Sharma T, McGuire PK. 1999. Methods for diagnosis and treatment of stimulus-correlated motion in generic brain activation studies using fMRI. Hum Brain Mapp 7:38–48.

Cox RW. 1996. AFNI: software for analysis and visualization of functional magnetic resonance neuroimages. Comput Biomed Res 29:162–173.

Fisher BE, Li Q, Nacca A, Salem GJ, Song J, Yip J, Hui JS, Jakowec MW, Petzinger GM. 2013. Treadmill exercise elevates striatal dopamine D2 receptor binding potential in patients with early Parkinson's disease. Neuroreport 24:509–514.

Fisher BE, Petzinger GM, Nixon K, Hogg E, Bremmer S, Meshul CK, Jakowec MW. 2004. Exercise-induced behavioral recovery and neuroplasticity in the 1-methyl-4-phenyl-1,2,3,6-tetrahydropyridine-lesioned mouse basal ganglia. J Neurosci Res 77:378–390.

Fisher BE, Wu AD, Salem GJ, Song J, Lin C-HJ, Yip J, Cen S, Gordon J, Jakowec M, Petzinger G. 2008. The effect of exercise training in improving motor performance and corticomotor excitability in people with early Parkinson's disease. Arch Phys Med Rehabil 89:1221–1229.

Göttlich M, Münte TF, Heldmann M, Kasten M, Hagenah J, Krämer UM. 2013. Altered resting state brain networks in Parkinson's disease. PLoS One 8:e77336.

Hacker CD, Perlmutter JS, Criswell SR, Ances BM, Snyder AZ. 2012. Resting state functional connectivity of the striatum in Parkinson's disease. Brain 135:3699–3711.

Helmich RC, Aarts E, de Lange FP, Bloem BR, Toni I. 2009. Increased dependence of action selection on recent motor history in Parkinson's disease. J Neurosci 29:6105–6113.

Helmich RC, Derikx LC, Bakker M, Scheeringa R, Bloem BR, Toni I. 2010. Spatial remapping of cortico-striatal connectivity in Parkinson's disease. Cereb Cortex 20:1175–1186.

Hoehn MM, Yahr MD. 1967. Parkinsonism: onset, progression and mortality. Neurology 17:427–442.

Jiang A, Kennedy DN, Baker JR, Weisskoff RM, Tootell RBH, Woods RP, Benson RR, Kwong KK, Brady TJ, Rosen BR, Belliveau JW. 1995. Motion detection and correction in functional MR imaging. Hum Brain Mapp 3:224–235.

Karvonen MJ, Kentala E, Mustala O. 1957. The effects of training on heart rate; a longitudinal study. Ann Med Exp Biol Fenn 35:307–315.

Lowe MJ. 2012. The emergence of doing ''nothing'' as a viable paradigm design. Neuroimage 62:1146–1151.

Lowe MJ, Beall EB, Sakaie KE, Koenig Ka, Stone L, Marrie RA, Phillips MD. 2008. Resting state sensorimotor functional connectivity in multiple sclerosis inversely correlates with transcallosal motor pathway transverse diffusivity. Hum Brain Mapp 29:818–827.

Lowe MJ, Dzemidzic M, Lurito JT, Mathews VP, Phillips MD. 2000. Correlations in low-frequency BOLD fluctuations reflect cortico-cortical connections. Neuroimage 12:582–587.

Lowe MJ, Mock BJ, Sorenson JA. 1998. Functional connectivity in single and multislice echoplanar imaging using resting-state fluctuations. Neuroimage 7:119–132.

Lowe MJ, Phillips MD, Lurito JT, Mattson D, Dzemidzic M, Mathews VP. 2002. Multiple sclerosis: low-frequency temporal blood oxygen level-dependent fluctuations indicate reduced functional connectivity initial results. Radiology 224:184–192.

Lowe MJ, Russell DP. 1999. Treatment of baseline drifts in fMRI time series analysis. J Comput Assist Tomogr 23:463–473.

Lowe MJ, Sorenson JA. 1997. Spatially filtering functional magnetic resonance imaging data. Magn Reson Med 37:723–729.

Luo C, Song W, Chen Q, Zheng Z, Chen K, Cao B, Yang J, Li J, Huang X, Gong Q, Shang H-F. 2014. Reduced functional connectivity in early-stage drug-naive Parkinson's disease: a resting-state fMRI study. Neurobiol Aging 35:431–441.

Mathew BA. Improved Methodology to Transform to Talairach Space Using Modified Template. In OHBM, Beijing, China, 2012, p. 7336.

Meissner WG, Frasier M, Gasser T, Goetz CG, Lozano A, Piccini P, Obeso JA, Rascol O, Schapira A, Voon V, Weiner DM, Tison F, Bezard E. 2011. Priorities in Parkinson's disease research. Nat Rev Drug Discov 10:377–393.

Nolte J. 2009. *The Human Brain: An Introduction to Its Functional Anatomy*, 6th ed. Philadelphia, PA: Mosby/Elsevier.

Palmer SJ, Eigenraam L, Hoque T, McCaig RG, Troiano A, McKeown MJ. 2009. Levodopa-sensitive, dynamic changes in effective connectivity during simultaneous movements in Parkinson's disease. Neuroscience 158:693–704.

Palmer SJ, Li J, Wang ZJ, McKeown MJ. 2010. Joint amplitude and connectivity compensatory mechanisms in Parkinson's disease. Neuroscience 166:1110–1118.

Petzinger GM, Fisher BE, McEwen S, Beeler JA, Walsh JP, Jakowec MW. 2013. Exercise-enhanced neuroplasticity targeting motor and cognitive circuitry in Parkinson's disease. Lancet Neurol 12:716–726.

Petzinger GM, Walsh JP, Akopian G, Hogg E, Abernathy A, Arevalo P, Turnquist P, Vucković M, Fisher BE, Togasaki DM, Jakowec MW. 2007. Effects of treadmill exercise on dopaminergic transmission in the 1-methyl-4-phenyl-1,2,3,6-tetrahydropyridine-lesioned mouse model of basal ganglia injury. J Neurosci 27:5291–5300.

Poston KL, Eidelberg D. 2012. Functional brain networks and abnormal connectivity in the movement disorders. Neuroimage 62:2261–2270.

Poulton NP, Muir GD. 2005. Treadmill training ameliorates dopamine loss but not behavioral deficits in hemi-parkinsonian rats. Exp Neurol 193:181–197.

Press WH, Teukolsky SA, Vetterling WT, Flannery BP. 2007. *Numerical Recipes 3rd Edition: The Art of Scientific Computing*. Cambridge: Cambridge University Press.

Ridgel AL, Vitek JL, Alberts JL. 2009. Forced, not voluntary, exercise improves motor function in Parkinson's disease patients. Neurorehabil Neural Repair 23:600–608.

Saad ZS, Glen DR, Chen G, Beauchamp MS, Desai R, Cox RW. 2009. A new method for improving functional-to-structural MRI alignment using local Pearson correlation. Neuroimage 44:839–848.

Sharman M, Valabregue R, Perlbarg V, Marrakchi-Kacem L, Vidailhet M, Benali H, Brice A, Lehéricy S. 2013. Parkinson's disease patients show reduced cortical-subcortical sensorimotor connectivity. Mov Disord 28:447–454.

Smidt N, de Vet HCW, Bouter LM, Dekker J, Arendzen JH, de Bie RA, Bierma-Zeinstra SM, Helders PJM, Keus SHJ, Kwakkel G, Lenssen T, Oostendorp RA, Ostelo RWJG, Reijman M, Terwee CB, Theunissen C, Thomas S, van Baar ME, van't Hul A, van Peppen RPS, Verhagen A, van der Windt DA; Exercise Therapy Group. 2005. Effectiveness of exercise therapy: a best-evidence summary of systematic reviews. Aust J Physiother 51:71–85.

Tajiri N, Yasuhara T, Shingo T, Kondo A, Yuan W, Kadota T, Wang F, Baba T, Tayra JT, Morimoto T, Jing M, Kikuchi Y, Kuramoto S, Agari T, Miyoshi Y, Fujino H, Obata F, Takeda I, Furuta T, Date I. 2010. Exercise exerts neuroprotective effects on Parkinson's disease model of rats. Brain Res 1310:200–207.

Thesen S, Heid O, Mueller E, Schad LR. 2000. Prospective acquisition correction for head motion with image-based tracking for real-time fMRI. Magn Reson Med 44:457–465.

Tillerson JL, Caudle WM, Reverón ME, Miller GW. 2003. Exercise induces behavioral recovery and attenuates neurochemical deficits in rodent models of Parkinson's disease. Neuroscience 119:899–911.

Wu T, Chan P, Hallett M. 2010. Effective connectivity of neural networks in automatic movements in Parkinson's disease. Neuroimage 49:2581–2587.

Wu T, Long X, Wang L, Hallett M, Zang Y, Li K, Chan P. 2011a. Functional connectivity of cortical motor areas in the resting state in Parkinson's disease. Hum Brain Mapp 32:1443–1457.

Wu T, Wang J, Wang C, Hallett M, Zang Y, Wu X, Chan P. 2012. Basal ganglia circuits changes in Parkinson's disease patients. Neurosci Lett 524:55–59.

Wu T, Wang L, Chen Y, Zhao C, Li K, Chan P. 2009. Changes of functional connectivity of the motor network in the resting state in Parkinson's disease. Neurosci Lett 460:6–10.

Wu T, Wang L, Hallett M, Chen Y, Li K, Chan P. 2011b. Effective connectivity of brain networks during self-initiated movement in Parkinson's disease. Neuroimage 55:204–215.

Yu R, Liu B, Wang L, Chen J, Liu X. 2013. Enhanced functional connectivity between putamen and supplementary motor area in Parkinson's disease patients. PLoS One 8: e59717.

Zigmond MJ, Cameron JL, Leak RK, Mirnics K, Russell VA, Smeyne RJ, Smith AD. 2009. Triggering endogenous neuroprotective processes through exercise in models of dopamine deficiency. Parkinsonism Relat Disord 15 Suppl 3: S42–S45.

Address correspondence to:
Chintan Shah
Department of Radiology
Hospital of the University of Pennsylvania
3400 Spruce Street, 1 Silverstein
Philadelphia, PA 19104

E-mail: shahc@uphs.upenn.edu

(*Appendix follows* →)

Appendix

Quality Assessment of Functional Connectivity Maps

Motion is especially problematic in functional connectivity magnetic resonance imaging (fcMRI), because there is no model for the expected signal, beyond restricting to low frequencies. This is of particular importance in movement disorders such as Parkinson's disease (PD), as patients with these disorders tend to move more than controls, as seen in previous studies (Göttlich et al., 2013; Helmich et al., 2010). Retrospective motion correction is imperfect, because current methods use a volumetric approach (Beall and Lowe, 2014). Accordingly, the effects of motion may be passed to the connectivity analysis. Visual inspection of the FC maps can be helpful in identifying corrupted maps. However, this is a difficult, subjective, time-intensive task. Here, we present an objective method for identifying FC maps likely to be of poor quality through statistical characterization of their *t*-score distributions.

z-Score correction is a method to correct for global effects that bias the *t*-score distribution. The FWHM of the *t*-score distribution is fit to a normal curve, and the fitted mean (μ_f) and standard deviation (σ_f) are used to center and normalize the distribution (Lowe et al., 1998). μ_f represents the average magnitude of the biasing effects, and σ_f is related to the spatial variability in those effects. Thus, FC maps with large σ_f values may contain artifacts unrelated to neuronal activity. The fit is restricted to the FWHM because this is assumed to be comprised primarily of Gaussian-distributed effects, or the null component. Meanwhile the tails contain higher order correlations that are non-null (Fig. A1) (Lowe et al.,1998), and may be of interest, though can also be produced by artifactual sources, such as motion. Information in the tails can be quantified by calculating the fifth standardized moment (γ) of the distribution [Eq. (A1)], which provides a characterization of asymmetry that is sensitive further from the mean (i.e., in the tail regions). It is our hypothesis that while motion artifact is highly variable in its effects, higher order characteristics of the *t*-score distribution are objectively sensitive and specific

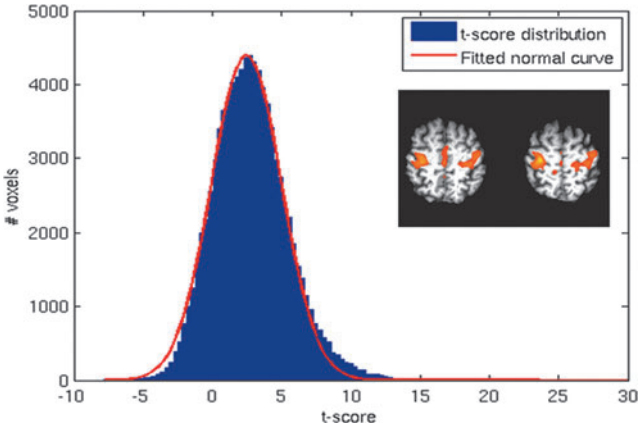

FIG. A1. Uncorrected *t*-score distribution of a functional connectivity (FC) map (inset). Note departure from normality in tail regions.

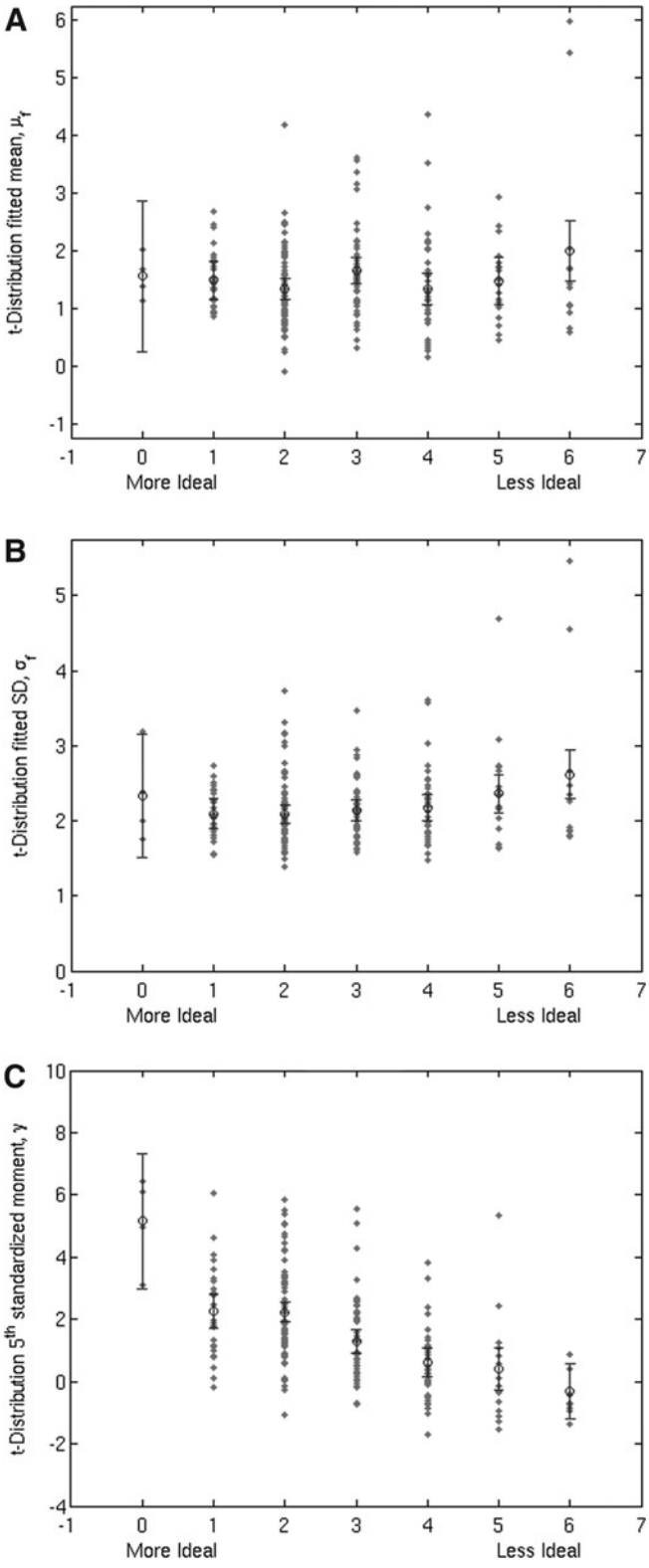

FIG. A2. Map quality ratings plotted against **(A)** μ_f, **(B)** σ_f, and **(C)** γ for task-related connectivity scans.

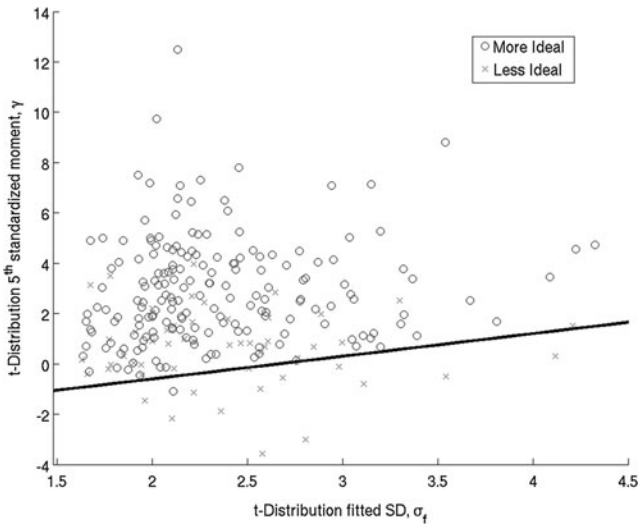

FIG. A3. Statistical descriptor space, σ_f versus γ, with linear separator superimposed for task-related connectivity scans.

to the effect of motion. Statistical distributions of μ_f, σ_f, and γ were examined to determine whether any relationship existed with visual assessment of the FC maps.

$$\gamma = \frac{\frac{1}{N}\sum_{i=1}^{N}(x_i - \bar{x})^5}{\left(\frac{1}{N}\sum_{i=1}^{N}(x_i - \bar{x})^2\right)^{5/2}} \tag{A1}$$

Functional connectivity (FC) data were analyzed from 116 task-related fcMRI scans and 118 resting-state fcMRI scans in 33 PD patients, including those in this study. Scans were similar to those described above, and also included a resting-state fcMRI scan with the parameters of scan 3 above, with the patient asked to rest comfortably with eyes closed. FC maps were generated for FC to the left and right M1, using the methods above. The resultant 468 FC maps were visually inspected and rated on a 7-point scale (0–6) for both presence of motion-related artifact and degree to which they resembled prototypical motor connectivity maps. A metric based on statistical descriptors was devised and optimized to isolate nonideal studies (rating 4–6).

Though μ_f or σ_f did not have a direct relationship with map quality, large σ_f was seen in poor maps (Fig. A2, panels A, B). There was a direct relationship between γ and map quality with poorer maps tending to have a more negative γ (Fig. A2, panel C). A two-dimensional statistical descriptor space between σ_f and γ was constructed, with poorer maps appearing primarily in the high- σ_f, low γ subspace. A linear separator was optimized to separate this subspace and separate poor maps (Fig. A3). For the task-related FC maps, 22 were separated out and 21 (95%) of these were rated as nonideal. For the resting-state FC maps, 13 of 14 separated maps (93%) were rated as nonideal.

Thus, *t*-score distributions that were either very broad or had heavy negative tails tended to be from poor FC maps. This is expected for a motor connectivity map, in which higher-order correlations should be mostly positive. Based on these statistical characteristics, a metric was created to objectively assess the quality of an FC map. The metric is not designed to be a highly sensitive test to identify all maps assessed as ''poor,'' and is not recommended to replace visual quality assessment. Rather, it is a specific test, with a high positive predictive value, that will provide objective criteria to exclude a map that is subjectively questionable.